Neurobiology of Aging 43 (2016) 58–71

Contents lists available at ScienceDirect

Neurobiology of Aging

journal homepage: www.elsevier.com/locate/neuaging

Sirt1 deficiency protects cochlear cells and delays the early onset of age-related hearing loss in C57BL/6 mice

Chul Han [a], Paul Linser [b], Hyo-Jin Park [c], Mi-Jung Kim [a], Karessa White [a], James M. Vann [d,e], Dalian Ding [f], Tomas A. Prolla [d,e], Shinichi Someya [a,*]

[a] Department of Aging and Geriatric Research, University of Florida, Gainesville, FL, USA
[b] Whitney Laboratory, University of Florida, St Augustine, FL, USA
[c] Department of Neurology, University of Florida, Gainesville, FL, USA
[d] Department of Genetics, University of Wisconsin, Madison, WI, USA
[e] Department of Medical Genetics, University of Wisconsin, Madison, WI, USA
[f] Center for Hearing and Deafness, State University of New York at Buffalo, NY, USA

ARTICLE INFO

Article history:
Received 16 April 2015
Received in revised form 29 February 2016
Accepted 22 March 2016
Available online 30 March 2016

Keywords:
Hearing loss
Aging
Inner ear
Oxidative stress
Sirtuin

ABSTRACT

Hearing gradually declines with age in both animals and humans, and this condition is known as age-related hearing loss (AHL). Here, we investigated the effects of deficiency of *Sirt1*, a member of the mammalian sirtuin family, on age-related cochlear pathology and associated hearing loss in C57BL/6 mice, a mouse model of early-onset AHL. *Sirt1* deficiency reduced age-related oxidative damage of cochlear hair cells and spiral ganglion neurons and delayed the early onset of AHL. In cultured mouse inner ear cell lines, *Sirt1* knockdown increased cell viability under oxidative stress conditions, induced nuclear translocation of Foxo3a, and increased acetylation status of Foxo3a. This resulted in increased activity of the antioxidant enzyme catalase. In young wild-type mice, both Sirt1 and Foxo3a proteins resided in the cytoplasm of the supporting cells within the organ of Corti of the cochlea. Therefore, our findings suggest that SIRT1 promotes early-onset AHL through suppressing FOXO3a-mediated oxidative stress resistance in the cochlea of C57BL/6 mice.

1. Introduction

Sirtuins are a family of NAD^+-dependent protein deacetylases that are known to extend life span in lower organisms (Finkel et al., 2009). Although earlier studies have shown that overexpression of sirtuins increases life span in lower organisms (Rogina and Helfand, 2004; Tissenbaum and Guarente, 2001; Viswanathan et al., 2005), later studies revealed that overexpression of sirtuin genes do not increase life span when compared with a genetically standardized control strain in worms and flies (Burnett et al., 2011). Caloric restriction (CR) extends life span and delays the onset of age-related diseases, including age-related hearing loss (AHL) in mammals (Someya et al., 2010; Weindruch and Sohal, 1997). Earlier studies showed that CR increases life span by activating sirtuins in yeasts, worms, or flies (Lin et al., 2000; Rogina and Helfand, 2004; Wang and Tissenbaum, 2006). These studies have led to the development of sirtuin activators as a potential strategy to delay aging and age-related diseases in humans (Baur et al., 2006). However, subsequent studies revealed that sirtuins are not required for life span extension by CR in these organisms (Kaeberlein, 2010; Kenyon, 2010). Furthermore, overexpression of *Sirt1*, a member of the mammalian sirtuin family, increases apoptotic cell death in hearts and decreases cardiac function in mice (Alcendor et al., 2007), whereas *Sirt1* inhibition protects rat cortical neurons against oxidative stress (Li et al., 2008). Hence, the roles of sirtuins in extending health span and life span have proved controversial.

Hearing gradually declines with age in mammals, and this condition is known as AHL (Gates and Mills, 2005; Yamasoba et al., 2013). Hearing loss is the third most prevalent chronic condition in older adults and affects 40% of people older than 65 years and 80% of people older than 85 years (Gates and Mills, 2005; Yamasoba et al., 2013). Hearing loss also affects speech understanding (Frisina and Frisina, 1997), contributes to isolation and depression, and has been linked to dementia. AHL arises from age-dependent loss of sensory hair cells, spiral ganglion neurons (SGNs), and/or stria vascularis atrophy in the cochlea of the inner ear. Hair cells are the sensory receptors that transduce sound stimuli into electrical responses (Hudspeth, 1997). The inner hair cells (IHCs) are the actual sensory receptors that relay their electrical response postsynaptically to the central auditory system through the auditory

* Corresponding author at: Department of Aging and Geriatric Research, University of Florida, 2004 Mowry Road, PO Box 112610, Gainesville, FL 32611, USA. Tel.: 352-294-5167; fax: 352-294-5058.
E-mail address: someya@ufl.edu (S. Someya).

0197-4580/$ – see front matter © 2016 Elsevier Inc. All rights reserved.
http://dx.doi.org/10.1016/j.neurobiolaging.2016.03.023

nerves or SGNs, whereas outer hair cells (OHCs) receive mostly efferent input. Stria vascularis is heavily vascularized and holds numerous capillary loops and small blood vessels that are essential for transporting oxygen, nutrients, and hormones into the cochlea. Hence, these cells are essential for maintaining auditory function, and extensive loss or degeneration of the hair cells or SGNs, and/or atrophy of the stria vascularis results in hearing loss.

We have shown previously that Sirt3, a mitochondrial sirtuin, is required for the CR-mediated reduction of oxidative damage in the cochlear hair cells and SGNs and prevention of AHL in C57BL/6 (B6) mice, a mouse model of early-onset AHL and one of the most widely used mouse models for the studies of aging (Someya et al., 2010). In the present study, we examined the effects of *Sirt1* deficiency on age-related cochlear pathology and associated hearing loss in B6 mice. Our results show that *Sirt1* deficiency reduces age-related oxidative damage of cochlear hair cells and SGNs and delays the early onset of AHL by enhancing Foxo3a-mediated oxidative stress resistance in the cochlea of B6 mice.

2. Materials and methods

2.1. Animals

Male and female *Sirt1*$^{+/-}$ mice were a gift from Dr. Frederick W. Alt (Harvard University Medical School, Boston, MA, USA) and have been described previously (Cheng et al., 2003). Details on the methods used to house and feed mice have been described previously (Pugh et al., 1999). Experiments were performed in accordance with protocols approved by the University of Wisconsin-Madison Institutional Animal Care and Use Committee. Only male wild-type (WT) and *Sirt1*$^{+/-}$ littermates were used in the present study.

2.2. Genotyping and DNA sequencing

Sirt1 genotyping: *Sirt1*$^{+/-}$ males were mated with *Sirt1*$^{+/-}$ females, and the offspring from these mating were genotyped from DNA obtained by a tail clip at weaning. The following primers were used for genotyping: SIRT1SKO-F 5′-CTTGCACTTCAAGGGACCAA-3′; SIRT1SKO-R1 5′-GTATACCCACCACATCTGAG-3′; SIRT1SKO-R2 5′-CTACCACTCCTGGCTACCAA-3′. The polymerase chain reaction (PCR) cycling parameters were as follows: 94 °C for 3 minutes; 35 cycles of 94 °C for 30 seconds, 56 °C for 60 seconds, 72 °C for 60 seconds; 72 °C for 10 minutes. PCR products were separated on 1.5% agarose gel, and the expected band size for WT and knockout (KO) allele were 500 and 800 bps, respectively (Fig. 1A).

Cdh23 genotyping: male and female *Sirt1*$^{+/-}$ mice have been backcrossed for 4 generations onto the C57BL/6J mouse strain that is homozygous for the recessive AHL-susceptibility allele *Cdh23*^{753A}. To confirm that both *Sirt1*$^{+/+}$ and *Sirt1*$^{+/-}$ mice have the same genotype for *Cdh23*, we amplified the DNA region containing the 753rd nucleotide in the *Cdh23* gene by PCR reaction and sequenced the *Cdh23* gene in the DNA obtained from tails of young *Sirt1*$^{+/+}$ and *Sirt1*$^{+/-}$ mice (N = 4 each group). The following primers were used for the PCR reaction: Cdh23-F 5′- GATCAAGACAAGACCA-GACCTCTGTC-3′; Cdh23-R 5′-GAGCTACCAGGAACAGCTTGGGCCTG-3′. The size of amplified PCR product was 360 bps. We confirmed that all the *Sirt1*$^{+/+}$ mice have the *Cdh23*$^{753A/753A}$ genotype, and all the *Sirt1*$^{+/-}$ mice have the *Cdh23*$^{753A/753A}$ genotype (Fig. 1B).

2.3. ABR hearing test

At 3 and 12 months of age, auditory brainstem responses (ABRs) were measured with a tone burst stimulus at 8, 16, and 32 kHz using an ABR recording system (Intelligent Hearing System, Miami, FL, USA) as previously described (Someya et al., 2010). Mice were anesthetized with a mixture of xylazine hydrochloride (10 mg/kg, i.m.; Phoenix Urology of St. Joseph, St. Joseph, MO, USA) and ketamine hydrochloride (40 mg/kg, i.m.; Phoenix Urology of St. Joseph). We used 9–12 mice per group for ABR hearing assessment. After the ABR hearing measurements, tissues from the same mice were used to conduct histopathological and biochemical analyses.

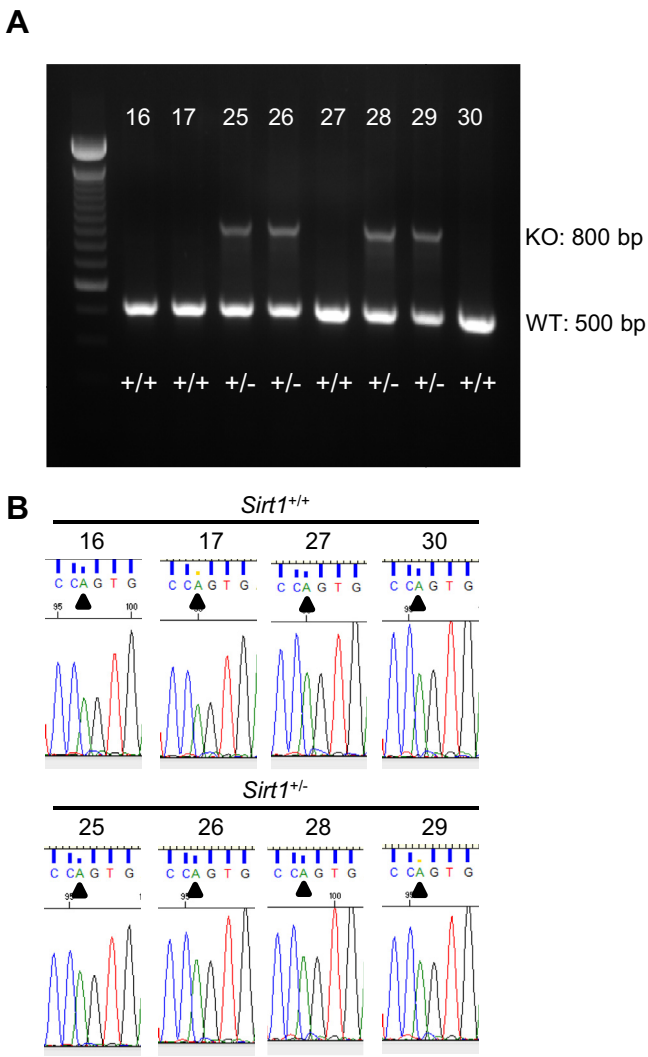

Fig. 1. Genotyping of *Sirt1*$^{+/+}$ and *Sirt1*$^{+/-}$ mice. (A) PCR products were separated on 1.5% agarose gel and the expected band sizes for WT and KO alleles were 500 and 800 bps, respectively. (B) The *Cdh23* gene in WT and *Sirt1*$^{+/-}$ mice (n = 4) was sequenced. All the *Sirt1*$^{+/+}$ mice had the *Cdh23*$^{753A/753A}$ genotype, and all the *Sirt1*$^{+/-}$ mice had the *Cdh23*$^{753A/753A}$ genotype. Arrows indicate the *Cdh23*^{753A} allele. Abbreviations: KO, knockout; PCR, polymerase chain reaction; WT, wild-type.

2.4. Cochlear histology

After the ABR hearing measurements, the animals were sacrificed by cervical dislocation, and the temporal bone was excised from the head and divided into cochlear and vestibular parts (Someya et al., 2010). The cochlea was then excised, immersed in a fixative containing 4% paraformaldehyde (Sigma-Aldrich, St. Louis, MO, USA) in phosphate-buffered saline solution for 1 day, and decalcified in 10% ethylenediaminetetraacetic acid for 1 week. The paraffin-embedded specimens were sliced into 4-μm sections, mounted on silane-coated slides, stained with hematoxylin and

eosin, and observed under a light microscope (Leica). The Rosenthal's canal was divided into 3 regions: apical, middle, and basal; and the 3 regions were used for evaluation of cochlear histology. We used 4–5 mice per group for histopathological assessment. In each mouse, we evaluated every third modiolar section obtained from 1 cochlea for a total of 10 sections. Tissues from the same animals were used for neuron counting, hair cell counting, and stria vascularis thickness measurement.

2.5. Cochlear cell counting

SGN counting: SGNs were counted in the apical, middle, and basal regions of the cochlear sections using a 40× objective as previously described (Someya et al., 2009). Ten sections of the apical, middle, and basal turns were evaluated in one cochlea per mouse. We used 4–5 mice per group for SGN counting. Hair cell counting: OHCs and IHCs were counted in the apical, middle, and basal regions of the cochlear sections using a 40× objective (Someya et al., 2009). Hair cells were identified by the presence of a nucleus. The OHC survival percentage was calculated as the number of intact OHCs present among the 3 OHCs that should be observed in each turn of one cochlea in tissue sections of mice with normal hearing. The IHC survival percentage was calculated as the number of intact IHCs present of the one IHC that should be observed in each turn of one cochlea in tissue sections of mice with normal hearing. Ten sections of the apical, middle, and basal turns were evaluated in one cochlea per mouse. We used 4–5 mice per group for OHC and IHC counting.

2.6. Stria vascularis thickness measurements

Stria vascularis thickness was measured in 40× images of hematoxylin and eosin-stained mouse cochlear tissues. In the ImageJ program, the measurement was made by using a cursor to draw a line from the margin of the stria to the junction of the basal cells with the spiral ligament halfway between the attachment of Reissner's membrane and the spiral prominence (Keithley et al., 2005). Measurements were made at the basal, middle, and apical regions of the cochlea for each mouse, and averages of each region were calculated for each mouse. Six to 9 sections of the apical, middle and basal turns were evaluated in 1 cochlea per mouse. We used 4 mice per group for stria vascularis thickness measurements.

2.7. Immunohistochemistry

For confocal-based immunohistochemistry, cochlear sections on slides were rehydrated and subjected to antigen retrieval (0.01 M NaCitrate pH 6.0 for 30 minutes at 60 °C), and then incubated in diluted primary antibodies (Sirt1, Foxo3a and CoxIV) over night at 4 °C. The following day, the slides were washed extensively and appropriate fluorescently labeled secondary antibodies (Jackson ImmunoResearch Laboratories, West Grove, PA, USA) were applied for 2 hours at 37 °C. The slides were then washed thoroughly and treated with DAPI (4′,6-diamidino-2-phenylindole, InVitrogen, Eugene, OR, USA) to visualize DNA, and/or COXIV to visualize mitochondria. Cover slips were mounted with 60% glycerol in tris-buffered saline containing p-phenylenediamine (to inhibit fluorescence quench). Preparations were viewed and digital images gathered with a Leica SP5 laser scanning confocal microscope. Figures were assembled using CorelDRAW 12 software. For light microscopy-based immunohistochemistry, cochlear sections were treated with anti-8-oxoguanine antibody (mouse monoclonal, 1:400 dilution; Abcam, Boston, MA, USA) to visualize 8-oxoguanine-positive cells or catalase antibody (mouse monoclonal, 1:50 dilution, Sigma-Aldrich) to visualize catalase-positive cells using the M.O.M kit (Vector laboratories, Burlingame, CA, USA). Catalase-positive cells and 8-oxoguanine-positive cells were counted in the apical, middle, and basal regions using a 40× objective and the Cell Counter plugin of the ImageJ software. The 8-oxoguanine-positive cell percentage was calculated as the number of 8-oxoguanine-positive cells out of the total number of OHC, IHC, or SG cell. The catalase-positive cell percentage was calculated as the number of catalase-positive cells of the total number of OHC, IHC, or SG cell. Six to 9 sections of the apical, middle, and basal turns were evaluated in one cochlea per mouse. We used 4 mice per group for 8-oxoguanine-positive or catalase-positive cell counting.

2.8. Isolation of cytosol, nuclei, and mitochondria

Dissected inner ears or cultured cells were homogenized using a tissue grinder (Wheaton dounce tissue grinder, Fisher Scientific, Pittsburgh, PA, USA) containing 1 mL of Tris buffer (10 mM Tris, 1-mM ethylenediaminetetraacetic acid, 320 mM sucrose, pH 7.4) on ice and then centrifuged at 720 G (3000 rpm) for 5 minutes at 4 °C to get a nuclear fraction (pellet). The supernatant was centrifuged at 12,000 G for 10 minutes at 4 °C to get a mitochondrial fraction (pellet) and a cytosolic fraction (supernatant). The pellets (nuclear fraction and mitochondrial fraction) were resuspended vigorously with 200 μL or 100 μL of 1% NP-40 buffer (50-mM Tris, 250-mM NaCl, 1% NP40, pH 7.4) and after 30 minutes of incubation on ice, were centrifuged at 12,000 G for 10 minutes at 4 °C. Lamin B1, voltage-dependent anion channel (VDAC), or glyceraldehyde-3-phosphate dehydrogenase (GAPDH) was used as a nuclear, mitochondrial, or cytosolic marker, respectively.

2.9. Western blotting

Fifty micrograms of total protein was fractionated by 10% of sodium dodecyl sulfate polyacrylamide gel electrophoresis and transferred to nitrocellulose membranes (Bio-rad, Hercules, CA, USA). Membranes were incubated with the primary antibody followed by the horseradish peroxidase-linked secondary antibody. A chemiluminescent detection reagent (ECL Prime, GE Healthcare Life Sciences, Logan, UT, USA) or the Odyssey infrared scanner (LiCor Biosciences, Lincoln, NE, USA) was used to visualize proteins. The band intensity was quantified using the ImageJ program, and the levels of each protein were normalized by loading controls.

2.10. Cell line

HEI-OC1, a cochlear cell line, was a gift from Dr. Federico Kalinec (Department of Head and Neck Surgery, UCLA) and was maintained in high-glucose DMEM (Life technologies, Grand Island, NY, USA) containing heat inactivated 10% fetal bovine serum (HyClone FBS, GE Healthcare Life Sciences, Logan, UT, USA) as previously described (Kalinec et al., 2003). The HEI-OC1 cell line was derived from long-term cultures of cochleas of Immortomouse that was derived from CBA/Ca X C57BL/10 (Charles River, http://www.criver.com/products-services/basic-research/find-a-model/immortomouse).

2.11. Gene knockdown

To generate siRNA-mediated knockdown cells, HEI-OC1 cells (3×10^5) were plated on a 6-well plate one day before transfection. siRNA (Origene, Rockville, MD, USA) targeted to mouse Sirt1 and scrambled siRNA were transfected with lipofectamine RNAi max (Life Technologies, Grand Island, NY, USA) according to manufacturer's instructions. After 5 days of incubation, the expression of Sirt1 protein was examined by Western blotting.

2.12. In vitro oxidative stress test

The *Sirt1* knockdown or control cells were replated on a 96-well plate (3×10^4/well) and treated with hydrogen peroxide at 0–2.8 mM for 2 hours. For cell viability measurements, after 22 hours, the media was replaced with DMEM containing 50 μg/mL neutral red (Sigma-Aldrich) as previously described (Someya et al., 2009). After 2 hours, 200 μL of a neutral red destaining solution composed of 50% ethanol, 49% deionized water, and 1% glacial acetic acid (Sigma-Aldrich) was added to each well. The 96-well plate was placed on a plate shaker for 1 hour, and the OD of the neutral red extract in each well was measured at 540 nm in a microplate spectrophotometer (BioTek, Winooski, VT, USA). Each condition was run in duplicate.

2.13. Catalase activity assay

Catalase activity was measured using the catalase assay kit (Sigma-Aldrich) according to the manufacturer's instructions. In brief, 25 μL of samples (5–10 μg protein/μL) was mixed with 50 μL of 1× assay buffer and 25 μL of 200-mM H_2O_2 solution and incubated for 2 minutes at room temperature. The reaction was stopped by adding a stop solution (15-mM sodium azide in water). Then, 10 μL of the 100 μL reaction mixture was mixed with 990 μL of the color reagent (150-mM potassium phosphate buffer, pH 7.0, containing 0.25-mM 4-aminoantipyrine and 2-mM 3,5-dichloro-2-hydroxybenzensulfonic acid) in a new tube by inversion. After 15 minutes of incubation for color development, the absorbance was measured at 520 nm in a spectrometer. Activity (μmol/min/mg protein or U/mg protein) was calculated using the equation "$\Delta\mu moles\ (H_2O_2) = A_{520}\ (Blank) - A_{520}\ (Sample)$."

2.14. Acetylation levels of Foxo3a

Sirt1-knockdown cells and control cells were fractionated by Tris buffer and 1% NP-40 buffer containing deacetylase inhibitors (10-mM nicotinamide and 500-nM trichostatin). Nuclear lysates from *Sirt1*-knockdown cells and control cells were immunoprecipitated using the Pierce Classic IP kit (Thermo Scientific, Waltham, MA, USA). One milligram of nuclear lysates were precleared by the control agarose resin, combined with 3 μg of anti-acetyl lysine antibody (mouse monoclonal, Abcam; Cat.#ab22550), and incubated on the shaker at 4 °C for 16 hours. The antibody and/or lysate sample was added to Protein A/G agarose resin in a spin column and incubated on the shaker at 4 °C for 1 hour. The column was centrifuged at 12,000 G for 10 minutes and washed by IP lysis and/or wash buffer and 1× conditioning buffer. Fifty μL of 2× sample buffer was then added to the column. The column was incubated at 100 °C for 5 minutes and centrifuged at 12,000 G for 10 minutes. To measure acetylation levels of Foxo3a, Western blotting was performed using the immunoprecipitated samples using anti-Foxo3a antibody (rabbit polyclonal, used at 1:1000 dilution, Cell Signaling, Beverly, MA, USA).

2.15. Antibodies

For confocal-based immunohistochemistry, primary antibodies used were as follows: Sirt1 (rabbit polyclonal, 1:50 dilution; Millipore, Bedford, MA, USA), Foxo3a (rabbit polyclonal, 1:200 dilution; Sigma-Aldrich), COX IV (mouse monoclonal, 1:100 dilution; Abcam). For Western blotting, primary antibodies used were as follows: Sirt1 (mouse monoclonal, 1:1000 dilution; Sigma-Aldrich), Foxo3a (rabbit polyclonal, 1:1000 dilution; Cell Signaling), Catalase (mouse monoclonal, 1:2000 dilution; Sigma-Aldrich), superoxide dismutase 2 (SOD_2; mouse monoclonal, 1:1000 dilution; Abcam), Lamin B1 (rabbit polyclonal, 1:2000 dilution; Abcam), VDAC (rabbit polyclonal, 1:1000 dilution; Cell Signaling), GAPDH (rabbit polyclonal, 1:5000 dilution; Abcam). Secondary antibodies used were as follows: Mouse (1:5000 dilution; GE Healthcare Life Sciences, Piscataway, NJ, USA) and rabbit (1:5000 dilution, GE Healthcare Life Sciences) secondary antibodies.

2.16. Statistical analysis

All statistical analyses were carried out by Student's *t*-test for 2 groups or by 1-way analysis of variance with post-Tukey multiple comparison tests for more than 3 groups using the Prism 4.0 statistical analysis program (GraphPad). All tests were 2-sided with statistical significance set at $p < 0.05$.

3. Results

3.1. Sirt1 deficiency delays the early onset of AHL in B6 mice

First, to investigate whether Sirt1 plays a role in maintaining auditory function or in AHL, we conducted ABR hearing tests in young and middle-aged WT and $Sirt1^{+/-}$ mice that have been backcrossed onto the C57BL/6J strain for 4 generations. Because $Sirt1^{-/-}$ mice exhibited developmental defects and infrequently survived postnatally (Cheng et al., 2003), only WT and $Sirt1^{+/-}$ mice were used in this study. To avoid obesity and other age-related diseases, the animals were not fed ad libitum but were fed a control diet providing 85%–90% of the average ad libitum food intake of these mice. We first confirmed that aging resulted in increased ABR hearing thresholds at the high (32 kHz), middle (16 kHz), and low (8 kHz) frequencies in middle-aged WT mice (Fig. 2, left), indicating AHL. Surprisingly, aging did not result in increased ABR hearing thresholds in middle-aged $Sirt1^{+/-}$ mice at the same frequencies tested (Fig. 2, right), and there were no differences in hearing levels between young and middle-aged $Sirt1^{+/-}$ mice at 32, 16, and 8 kHz. $Sirt1^{+/-}$ mice were viable and fertile, and there were no differences in body weight between WT and $Sirt1^{+/-}$ mice at 3 or 12 months of age (data not shown).

3.2. Sirt1 deficiency protects cochlear hair cells and neurons

AHL arises from age-related loss of sensory hair cells, SGNs, and/or atrophy of the stria vascularis within the cochlea (Gates and Mills, 2005; Spongr et al., 1997; Yamasoba et al., 2013). To validate the ABR hearing test results, we performed histological analysis on cochlear tissue sections from young and middle-aged WT and $Sirt1^{+/-}$ mice. In agreement with the hearing test results, basal regions of the cochleas from young WT and $Sirt1^{+/-}$ mice displayed no or only minor loss of sensory IHCs, OHCs (Fig. 3A, B, E, and F), or SGNs (Fig. 3C and G) and no or only minor degeneration of strial vascularis cells (Fig. 3D and H). In middle-aged mice, basal regions of the cochleas from WT mice displayed severe loss of OHC and IHCs (Fig. 3I and J) and SGNs (Fig. 3K), whereas basal regions of the cochleas from age-matched $Sirt1^{+/-}$ mice displayed only minor loss or degeneration of these hair cells, SGNs (Fig. 3M–O), and increased stria vascularis thickness (Fig. 3P) when compared with WT mice (Fig. 3L).

To confirm the histological observation results, we counted the numbers of cochlear hair cells and SGNs and measured the thickness of stria vascularis of WT and $Sirt1^{+/-}$ mice at 3 and 12 months of age. *Sirt1* deficiency increased the survival of OHCs (Fig. 4A) and SGNs (Fig. 4C) and increased stria vascularis thickness (Fig. 4D) in the basal regions of the cochlea. However, no significant changes between WT and $Sirt1^{+/-}$ mice were observed in the survival of IHCs in the basal region at 12 months of age (Fig. 4B). At 3 months of

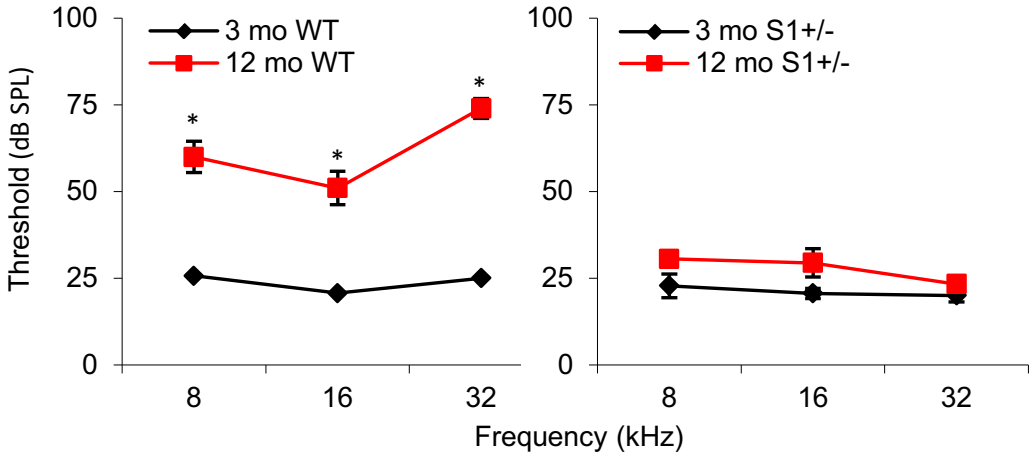

Fig. 2. *Sirt1* deficiency delays the early onset of age-related hearing loss. ABR hearing thresholds were measured at 32, 16, and 8 kHz from WT (left) and *Sirt1*$^{+/-}$ (right) mice at 3 and 12 months of age. *Significantly different from 3-month-old WT mice ($p < 0.05$). Data are means ± SEM. S1 = Sirt1. Abbreviations: ABR, auditory brainstem response; SEM, standard error of mean; WT, wild-type.

age, no significant changes between WT and *Sirt1*$^{+/-}$ mice were observed in the survival of OHCs, IHCs, or SGNs, or stria vascularis thickness in the basal cochlear regions (Fig. 4A–D). In the apical or middle cochlear regions, no significant changes between WT and *Sirt1*$^{+/-}$ mice were observed in the survival of IHCs or SGNs at 3 or 12 months of age (Fig. 4B and C). Collectively, these results

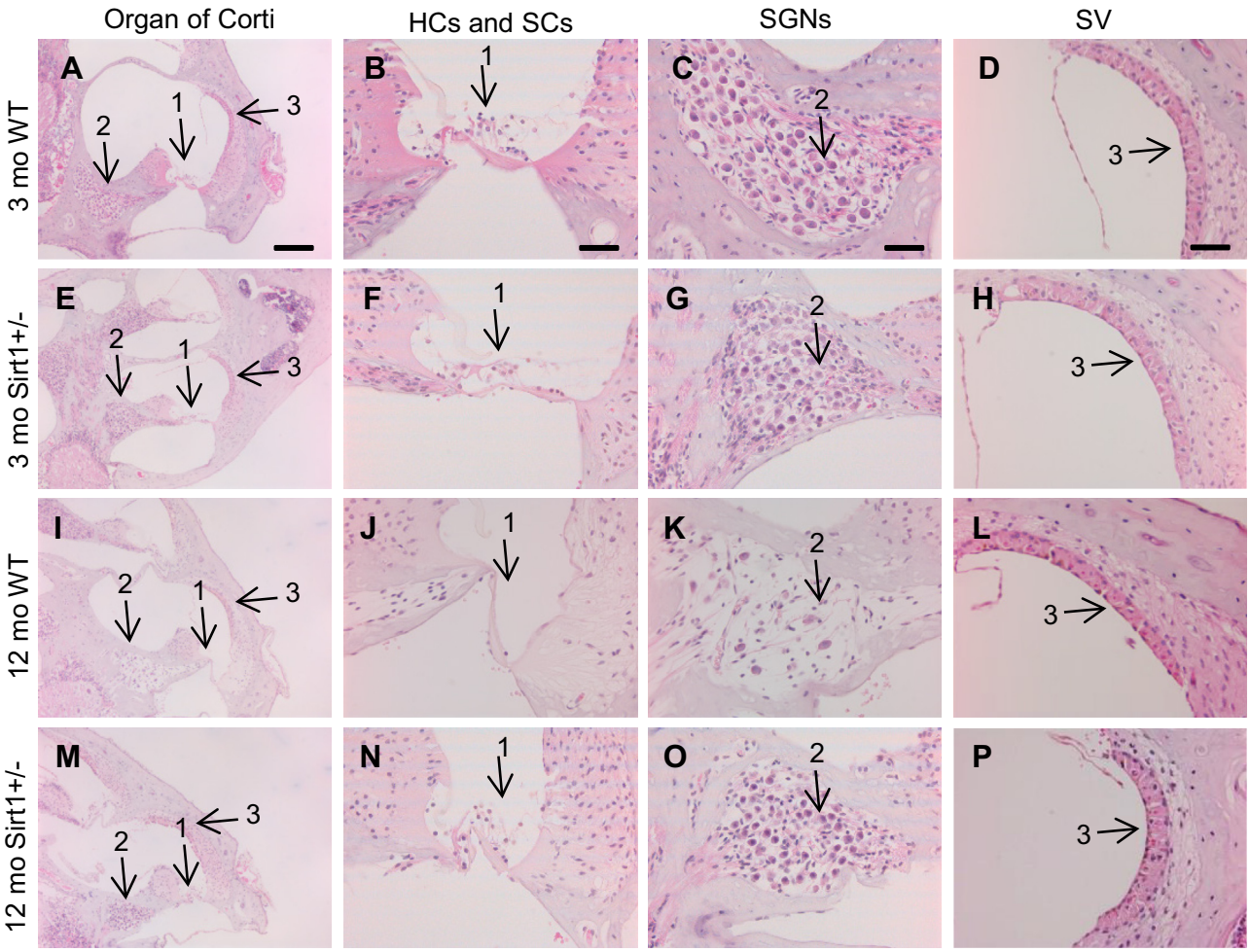

Fig. 3. *Sirt1* deficiency protects cochlear cells. Organ of Corti in the basal cochlear regions from 3-month-old WT (A) and *Sirt1*$^{+/-}$ (E) and 12-month-old WT (I) and *Sirt1*$^{+/-}$ (M) mice. Hair cells and SCs in the organ of Corti in the basal cochlear regions from 3-month-old WT (B) and *Sirt1*$^{+/-}$ (F) and 12-month-old WT (J) and *Sirt1*$^{+/-}$ (N) mice. SGNs in the basal cochlear regions from 3-month-old WT (C) and *Sirt1*$^{+/-}$ (G) and 12-month-old WT (K) and *Sirt1*$^{+/-}$ (O) mice. SV in the basal cochlear regions from 3-month-old WT (D) and *Sirt1*$^{+/-}$ (H) and 12-month-old WT (L) and *Sirt1*$^{+/-}$ (P) mice. Arrows 1 indicate HC and SC. Arrows 2 indicate SGN regions. Arrows 3 indicate SV regions. Scale bar = 100 μm (A) or 20 μm (B–D). Abbreviations: HCs, hair cells; SCs, supporting cells; SGNs, spiral ganglion neurons; SV, strial vascularis; WT, wild-type.

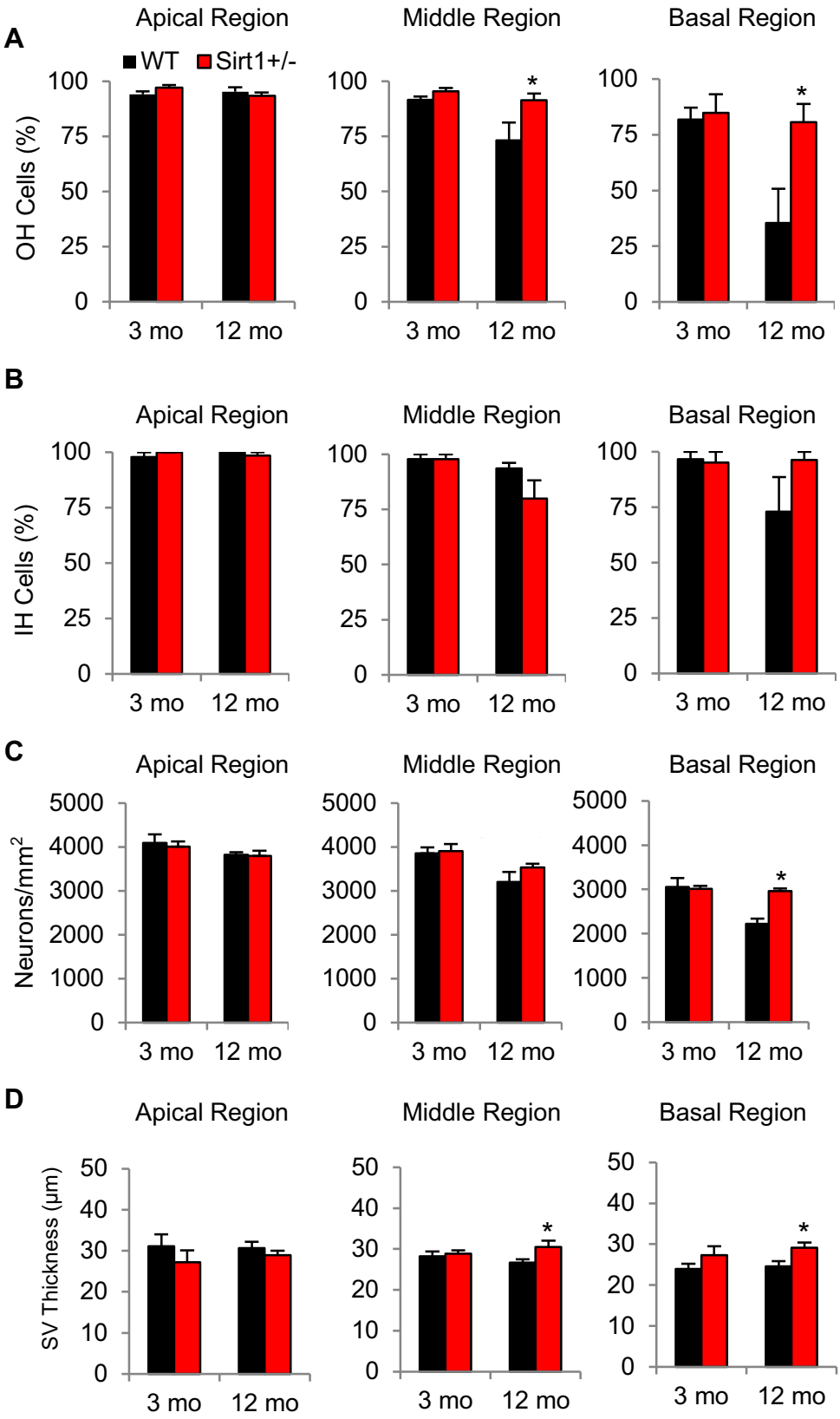

Fig. 4. *Sirt1* deficiency reduces age-related loss of HCs and SGNs in the cochlea. (A) OH cell survival (%) of apical, middle, and basal cochlear regions of WT and *Sirt1*$^{+/-}$ mice was measured at 3 and 12 months of age (n = 5). (B) IH cell survival (%) of apical, middle, and basal cochlear regions of WT and *Sirt1*$^{+/-}$ mice was measured at 3 and 12 months of age (n = 5). (C) SGN survival (SGN density) of apical, middle, and basal cochlear regions of WT and *Sirt1*$^{+/-}$ mice was measured at 3 and 12 months of age (n = 5). (D) SV thickness of apical, middle, and basal cochlear regions of WT and *Sirt1*$^{+/-}$ mice was measured at 3 and 12 months of age (n = 5). *Significantly different from 12-month-old WT mice ($p < 0.05$). Abbreviations: HCs, hair cells; IH, inner hair; OH, outer hair; SGNs, spiral ganglion neurons; SV, strial vascularis; WT, wild-type.

demonstrate that *Sirt1* deficiency protects cochlear OHCs and SGNs and delays the early onset of AHL in B6 mice.

3.3. *Sirt1* deficiency protects cochlear hair cells and neurons from oxidative stress

It is well documented that oxidative damage contributes to age-related loss of sensory hair cells, SGNs, and/or atrophy of the stria vascularis within the cochlea in mammals (Yamasoba et al., 2013). Hence, we hypothesized that *Sirt1* deficiency may protect cochlear sensory hair cells and neurons through the reduction of oxidative damage in the cochlea. To test this hypothesis, 8-oxoguanine, a common oxidative nuclear DNA damage marker, was immunostained with anti-8-oxoguanine antibody and observed under light microscopy. We found that middle-aged *Sirt1*$^{+/-}$ mice displayed significantly fewer 8-oxoguanine-positive cells in the OHCs and SGNs in the middle cochlear regions when compared with age-matched WT mice (Fig. 5D and E). In the apical cochlear regions, middle-aged *Sirt1*$^{+/-}$ mice also displayed significantly fewer 8-oxoguanine-positive cells in the IHCs, OHCs, and SGNs when compared with age-matched WT mice (Fig. 5A–C). In the basal cochlear regions, middle-aged *Sirt1*$^{+/-}$ mice displayed significantly fewer 8-oxoguanine-positive cells in the SGNs when compared to age-matched WT mice (Fig. 5G). At 3 months of age, no significant changes were observed in the numbers of 8-oxoguanine-positive cells in the OHCs, IHCs, or SGNs between WT and *Sirt1*$^{+/-}$ mice (Fig. 5A–G).

To further confirm the roles of Sirt1 in oxidative stress resistance of cochlear cells, we conducted in vitro oxidative stress tests using hydrogen peroxide (H_2O_2), followed by cell viability tests in cultured mouse inner ear cell lines (HEI-OC1) that were transfected with siRNA targeted to mouse *Sirt1*. We first confirmed that treatment with siRNA reduced Sirt1 protein expression levels by 67% compared with controls (treatment with scrambled siRNA) in the HEI-OC1 cells (Fig. 5H). Hydrogen peroxide reduced cell viability in a dose-dependent manner in the control cells; however, *Sirt1* knockdown cells displayed increased cell viability at multiple concentrations of H_2O_2 compared with control cells (Fig. 5I). Collectively, these results demonstrate that *Sirt1* deficiency protects cochlear hair cells and neurons from oxidative stress.

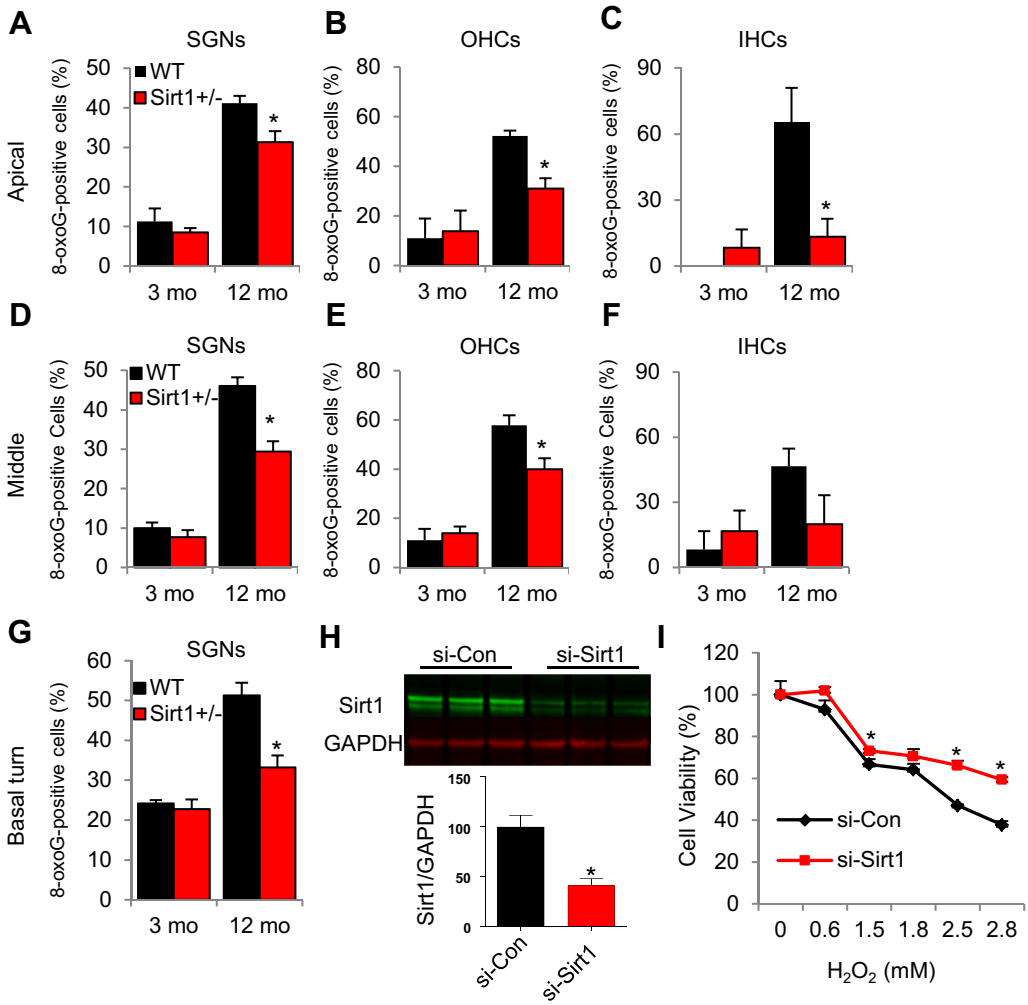

Fig. 5. *Sirt1* deficiency reduces oxidative nuclear DNA damage in the cochlea, whereas *Sirt1* knockdown increases cell viability in cultured mouse inner ear cells under oxidative stress conditions. (A–G) The numbers of 8-oxoguanine-positive cells were counted in the OHC (B and E), IHC (C and F), and SGNs (A, D, and G) in the apical (A–C), middle (D–F), and basal (G) cochlear regions from WT and *Sirt1*$^{+/-}$ mice at 3 and 12 months of age. *Significantly different from age-matched WT mice ($p < 0.05$). Data are means ± SEM. (H) Western blotting analysis of Sirt1 protein levels in *Sirt1* knockdown mouse inner ear cells (si-Sirt1) and control cells (si-Con): Quantification of Sirt1 proteins (lower panel) from (upper panel). (I) *Sirt1* knockdown increased the viability of cultured mouse inner ear cells treated with hydrogen peroxide (H_2O_2; n = 3; 0–2.8 mM). *Significantly different from control cells ($p < 0.05$). Abbreviations: IHC, inner hair cells; OHC, outer hair cells; SEM, standard error of mean; SGNs, spiral ganglion neurons; WT, wild-type.

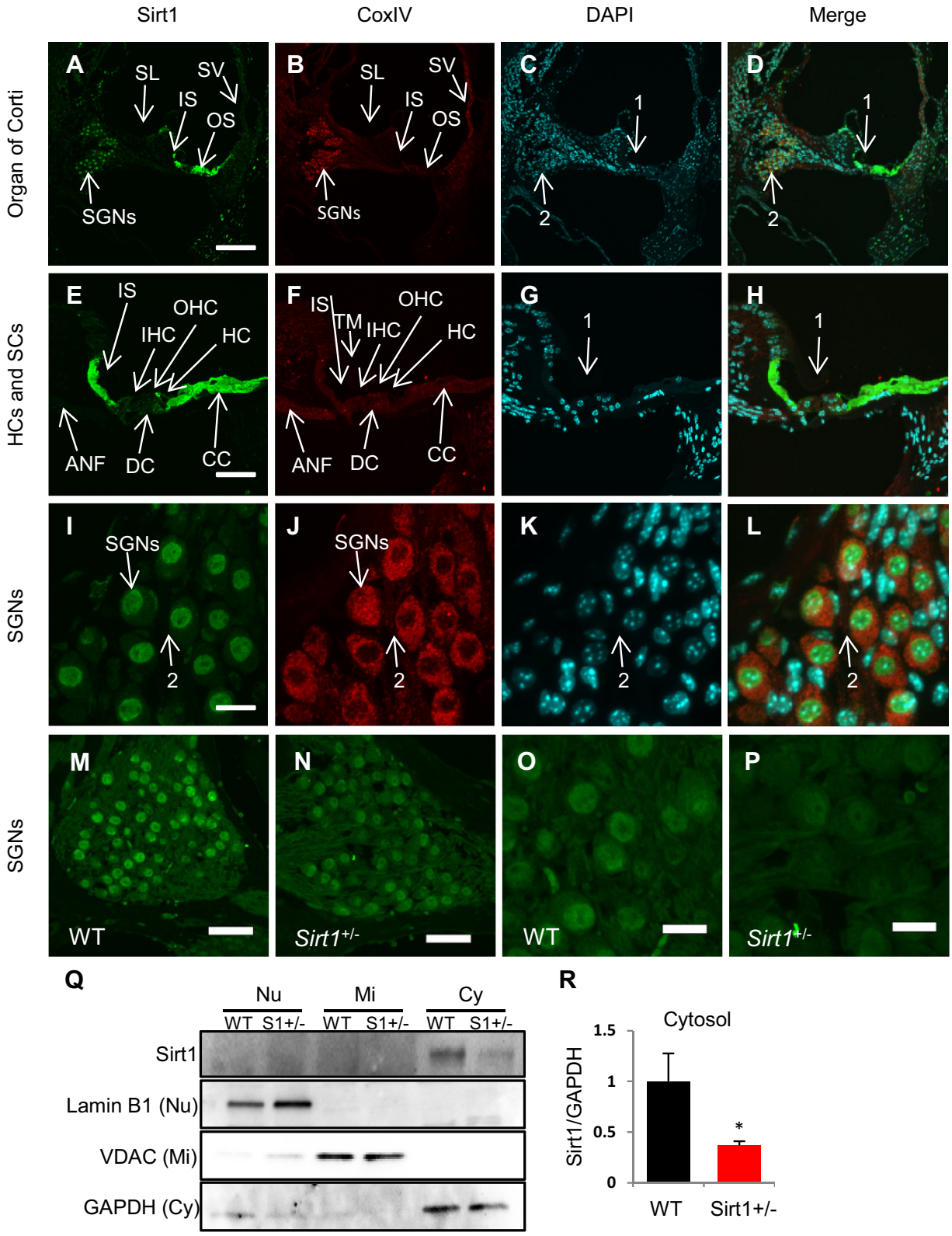

Fig. 6. Sirt1 is prominently localized in the cytosol of the supporting cells of the organ of Corti within the cochlea. (A–L) Sirt1 staining (green; A, E, and I), COX IV staining (mitochondrial marker; red; B, F, and J), DAPI staining (Nu marker; C, G, and K), and merged staining (D, H, and L) were detected in the organ of Corti regions (A–D), hair cells and their SCs (E–H), or SGNs (I–L) from 3-month-old WT mice. Arrows indicate hair cells and SCs in the organ of Corti region. Arrows 2 indicate SGNs. Figures were taken from the basal turn (A–H). Scale bar = 200 μm (A), 50 μm (E), or 15 μm (I). (M–P) Sirt1 staining in the SGN regions of WT (M and O) and *Sirt1*$^{+/-}$ (N and P) mice. Scale bar = 40 μm (M–N) or 15 μm (O–P). (Q and R) Western blotting analysis of Sirt1 protein levels in the cochlea from 3-month-old WT mice: Quantification of Sirt1 proteins in the Cy (R) from (Q). Lamin B1, VDAC, and GAPDH were used as a Nu, mitochondrial, and cytosolic markers, respectively. *Significantly different from WT mice ($P < 0.05$). Abbreviations: ANF, auditory nerve fibers; CC, Claudius cell; Cy, cytosol; DC, Deiters' cell; HC, Hensen's cell; IHC, inner hair cells; IS, inner sulcus cells; Mi, mitochondria; Nu, nuclear; OHC, outer hair cells; OS, outer sulcus region; SC, supporting cell; SGN, spiral ganglion neurons; SL, spiral lympus; SV, stria vascularis; S1, Sirt1; TM, tectorial membrane; WT, wild-type. (For interpretation of the references to color in this figure legend, the reader is referred to the Web version of this article.)

3.4. Sirt1 resides in the cytosol of the supporting cells within the organ of Corti of the cochlea

To investigate the localization of Sirt1 in the cochlea of young WT mice, Sirt1 was immunostained with anti-Sirt1 antibody and observed by confocal microscopy. Fig. 6A–D show an area of the organ of Corti in the cochlea at low magnification: Sirt1 immunostaining was detected as a very strong signal in the cytosol of some of the supporting cells of the organ of Corti, including the cells of Claudius (Fig. 6E–H) that provide mechanical support to the OHCs, and inner sulcus cells that enclose the sensory IHCs (Merchant and Nadol, 2010). There was also a signal for Sirt1 immunostaining in the nuclei of the neuronal cells of the spiral ganglion (Fig. 6I–L). When comparing signal intensities for the Sirt1 immunolocalization between WT and *Sirt1*$^{+/-}$ cochlear tissues, the SGNs from the *Sirt1*$^{+/-}$ mice clearly showed a lower level of Sirt1 than the WT (Fig. 6M–P). All conditions for labeling and imaging were identical, and the images were gathered on the same day using confocal settings first optimized for the WT and then used on the *Sirt1*$^{+/-}$ cochlear tissues. To confirm these immunostaining results, we performed Western blotting to measure Sirt1 protein levels in the cytosol, nuclei, and mitochondria in the inner ear tissues from 3 to 4-month-old WT and *Sirt1*$^{+/-}$ mice. We found that Sirt1 protein was expressed in the cytosol in the cochleas of WT mice (Fig. 6Q),

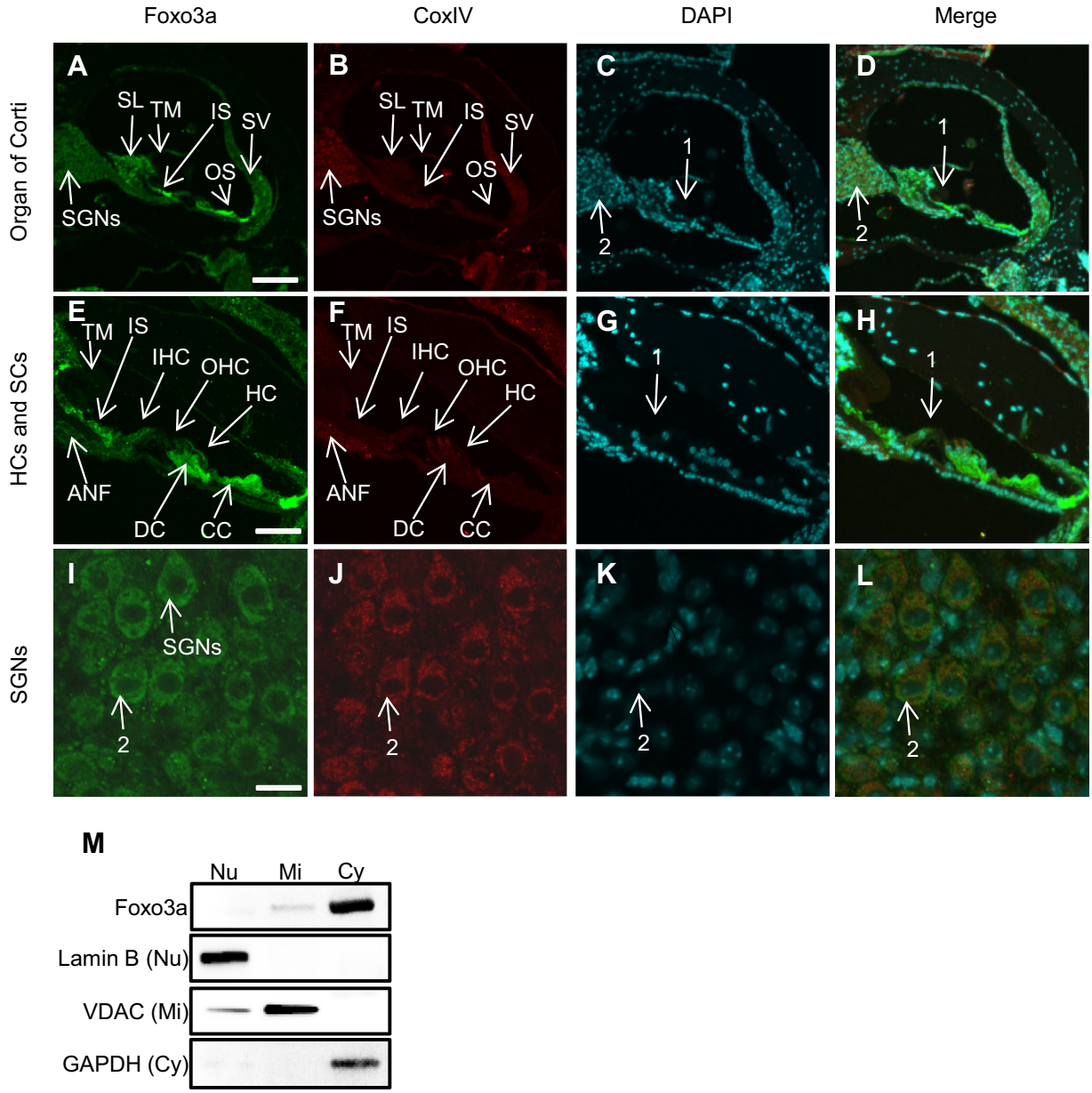

Fig. 7. Foxo3a is prominently localized in the cytosol of the supporting cells of the organ of Corti within the cochlea. (A–L) Foxo3a staining (green; A, E, and I), CoxIV staining (mitochondrial marker; red; B, F, and J), DAPI staining (Nu marker; C, G, and K), and merged staining (D, H, and L) were detected in the organ of Corti regions (A–D), hair cells and their SCs (E–H), or SGNs (I–L) from 3-month-old WT mice. Arrows 1 indicate hair cells and SCs in the organ of Corti region. Arrows 2 indicate SGNs. Figures were taken from the apical turn (A–H). Scale bar = 200 μm (A), 50 μm (E), or 15 μm (I).(M) Western blotting analysis of Foxo3a protein levels in the cochlea from 3-month-old WT mice. Lamin B, VDAC, and GAPDH were used as nuclear, mitochondrial, and cytosolic markers, respectively. Abbreviations: ANF, auditory nerve fibers; CC, Claudius cell; Cy, cytosol; DC, Deiters' cell; IHC, inner hair cells; IS, inner sulcus cells; HC, Hensen's cell; Mi, mitochondria; Nu, nuclear; OHC, outer hair cells; OS, outer sulcus region; SC, supporting cells; SGN, spiral ganglion neurons; SL, spiral lympus; SV, stria vascularis; TM, tectorial membrane; WT, wild-type. (For interpretation of the references to color in this figure legend, the reader is referred to the Web version of this article.)

whereas *Sirt1*$^{+/-}$ mice displayed a 63% decrease in Sirt1 protein levels in the cytosol of the cochlea compared with WT mice (Fig. 6R). Together, these results demonstrate that Sirt1 is expressed in the cochlea and resides in the cytosol of the supporting cells within the organ of Corti, including Claudius and inner sulcus cells.

3.5. *Foxo3a resides in the cytosol of the supporting cells within the organ of Corti of the cochlea*

The forkhead transcription factor FOXO3a regulates oxidative stress resistance by directly binding to the promoters of the antioxidant genes encoding catalase or manganese SOD in a variety of species (Calnan and Brunet, 2008; Huang and Tindall, 2007). Earlier studies have shown that Sirt1 directly inhibits Foxo3a activity by deacetylating Foxo3a in mammalian cells (Motta et al., 2004). Hence, we hypothesized that *Sirt1* deficiency may result in the activation of Foxo3a, which in turn activates catalase or SOD_2, thereby reducing oxidative stress in the cochlear hair cells and their supporting cells. To test this hypothesis, we first investigated the localization of Foxo3a proteins in the cochlea of young WT mice using confocal microscopy. Fig. 7A–D show an area of the organ of Corti in the cochlea at low magnification: Foxo3a immunostaining was detected as a very strong signal in the cytosol of some of the supporting cells of the organ of Corti, including Claudius cells, Deiters' cells that hold the basal end of the OHCs, and inner sulcus cells (Fig. 7E–H; Merchant and Nadol, 2010). IHC and OHC were also labeled but to a lesser extent than the supporting cells within the organ of Corti. The large neurons of the spiral ganglion and cells of the stria vascularis also exhibited staining (Fig. 7A–D and I–L). In all cases, cytosolic staining was apparent. If nuclear staining was present, it was minimal compared with the cytoplasmic staining within the same cell. To confirm these immunostaining results, we performed Western blotting to measure Foxo3a protein levels in the cytosol, nuclei, and mitochondria in the inner ear tissues from 3 to 4 months old WT mice. We found that Foxo3a proteins were expressed in the cytosol in the cochlear cells of WT mice (Fig. 7M). Together, these observations demonstrate that Foxo3a is expressed in the cochlea, and both Foxo3a and Sirt1 reside in the cytosol of the supporting cells within the organ of Corti, including Claudius and inner sulcus cells.

3.6. *Sirt1 deficiency activates Foxo3a and increases catalase activity in cochlear hair cells*

In response to external or internal stimuli or when activated through post-translational modifications such as acetylation, Foxo3a proteins translocate to the nucleus and bind to its targeted genes (Calnan and Brunet, 2008; Huang and Tindall, 2007). Hence, we hypothesized that *Sirt1* deficiency or knockdown may promote the translocation of Foxo3a to the nucleus where Foxo3a can directly bind and activate catalase or SOD_2 within the cochlea. To test this hypothesis, we first performed Western blotting to measure Foxo3a protein levels in the nuclei and cytosol in the HEI-OC1 cells that were transfected with siRNA targeted to mouse *Sirt1*. We found that *Sirt1* knockdown significantly increased nuclear Foxo3a protein levels when compared with control cells (Fig. 8A and B). Next, to investigate whether *Sirt1* knockdown increases the acetylation status of nuclear Foxo3a, we measured the acetylation levels of Foxo3a in the nuclei of siRNA-mediated *Sirt1* knockdown mouse inner ear cells. We found that *Sirt1* knockdown induced a 2.46-fold increase in acetylation (Fig. 8C and D).

Earlier studies have shown that when activated, Foxo3a directly binds to the promoters of the genes encoding catalase and SOD_2 in the nuclei (Calnan and Brunet, 2008; Huang and Tindall, 2007). To test the hypothesis that *Sirt1* knockdown increases the activity of catalase or SOD_2, we measured the protein levels of catalase and SOD_2 in siRNA-mediated *Sirt1* knockdown mouse inner ear cells. We found that *Sirt1* knockdown increased the protein levels of catalase but not SOD_2 (Fig. 8E and F). We then measured the activity of catalase in siRNA-mediated *Sirt1* knockdown mouse inner ear cells. We found that *Sirt1* knockdown significantly increased catalase activity in mouse inner ear cells (Fig. 8G). To confirm the siRNA-mediated *Sirt1* knockdown test results in mouse cochlear tissues, immunostaining of catalase was performed with anti-catalase antibody and observed by light microscopy. We found that middle-aged *Sirt1*$^{+/-}$ mice displayed significantly more catalase-positive cells in the IHCs, OHCs, and SGNs in the apical and middle cochlear regions when compared with age-matched WT mice (Fig. 8H–M). At 3 months of age, no significant changes were observed in the numbers of the catalase-positive cells in IHCs, OHCs, or SGNs between WT and *Sirt1*$^{+/-}$ mice (Fig. 8H–M). Collectively, these results demonstrate that *Sirt1* deficiency promotes the translocation of Foxo3a to the nucleus where it activates catalase in the sensory hair cells in the organ of Corti of the cochlea.

4. Discussion

4.1. *Sirt1 plays a role in early onset of AHL in C57BL/6 mice*

It has been proposed that sirtuins play an essential role in extending health span and life span in mammals (Finkel et al., 2009). In agreement with this idea, there is a significant reduction of Sirt1 expression in mouse cochlea and auditory cortex during aging (Xiong et al., 2014), whereas inhibition of Sirt1 leads to an increase in apoptosis in the mouse inner ear cell line (HEI-OC1; Xiong et al., 2015). Xiong et al. (2014) have also shown that Sirt1 protein was strongly expressed in the nuclei of the IHCs and weakly expressed in the OHCs. In the present study, however, Sirt1 was detected as a very strong signal in the cytosol of some of the supporting cells within the organ of Corti. We note that because the report by Xiong et al. did not provide information on Sirt1 expression in the supporting cells of the organ of Corti or a low magnification image of the organ or Corti, it is not clear whether Sirt1 was detected in the supporting cells in their study. We speculate that the discrepancy between their study and our study may be due to different antibodies and/or different microscopy used: our study used confocal microscopy which can provide finer details that cannot be detected in a nonconfocal, standard fluorescent microscope. In the present study, we also verified antibody specificity using cochlear tissues of *Sirt1*$^{+/-}$ mice and verified our Sirt1 sub-cellular localization result by measuring Sirt1 protein levels in the nuclei, cytosol, and mitochondria of the cochlear tissues by Western blot.

We were also unable to verify the antiaging effects of Sirt1 on AHL in mice. Indeed, our study suggests that Sirt1 may have an opposing role in promoting at least one feature of mammalian aging, AHL. Importantly, the current studies were conducted in the same animal facility using the same dietary feeding protocol and mouse genetic background as those of our previous *Sirt3* KO mouse study (Someya et al., 2010): both *Sirt1*$^{+/-}$ and *Sirt3*$^{-/-}$ mice were backcrossed onto the C57BL/6 mouse strain for 4 generations, and hence, the *Sirt1* and *Sirt3* KO mouse studies were conducted on the same genetic background. In both studies, animals were individually housed in the same mouse room and received the same diets. In the *Sirt3* KO mouse study, both 12-month-old WT and *Sirt3*$^{-/-}$ mice displayed AHL. In contrast, in the present study, we found that 12-month-old *Sirt1*$^{+/-}$ mice maintained normal hearing at the middle and high frequencies, while age-matched WT mice displayed AHL, indicating that Sirt1 plays a key role in early-onset AHL. Hence, these 2 independent studies provide strong evidence that under the

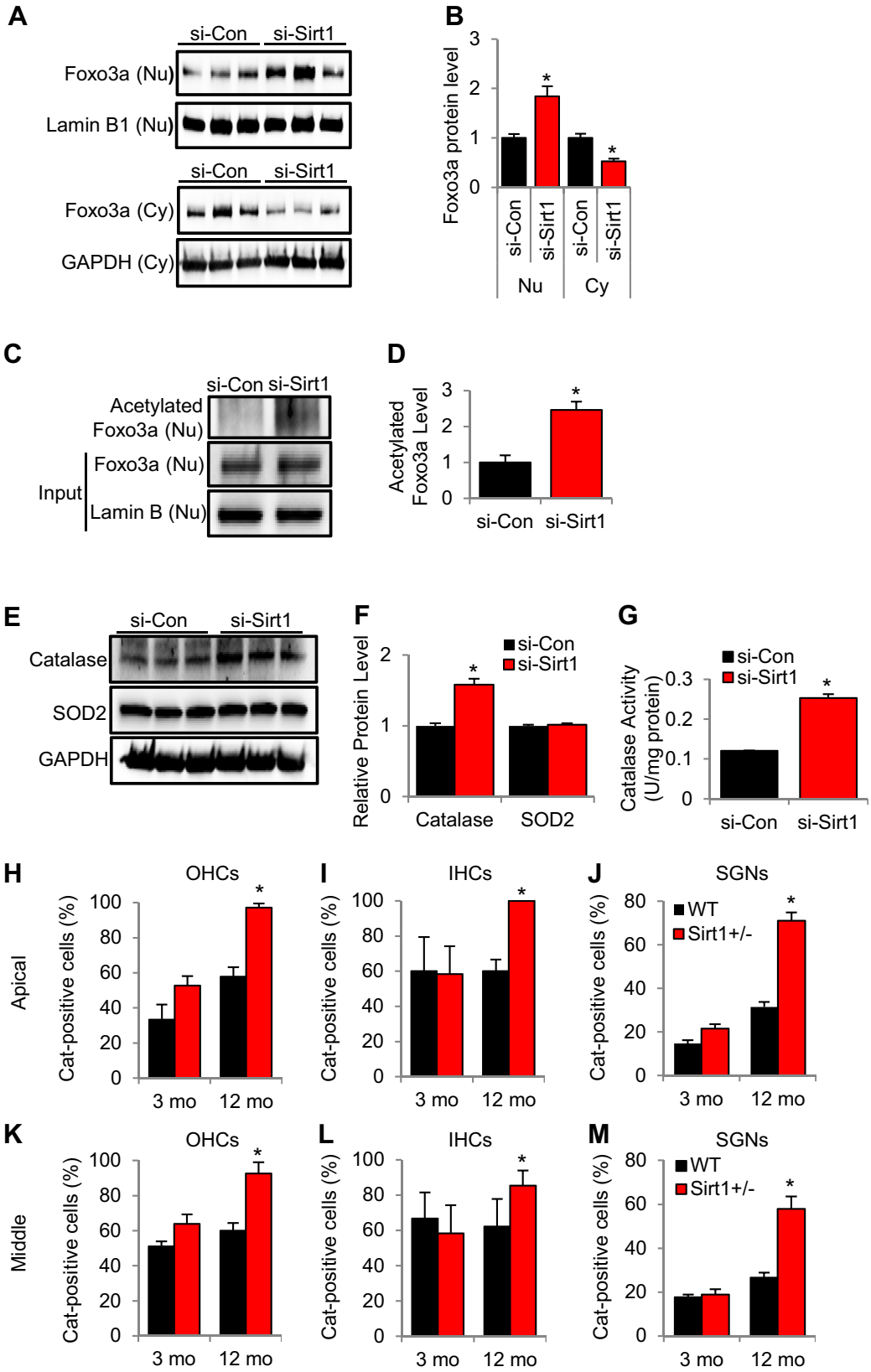

Fig. 8. *Sirt1* knockdown or deficiency activates Foxo3a and increases catalase activity in the cochlear sensory cells. (A and B) Western blotting analysis of Foxo3a protein levels in *Sirt1*-knockdown HEI-OC1 cells (si-Sirt1). (B) Quantification of Foxo3a proteins in the nuclei and Cy from (A). *Significantly different from control cells (si-Con; $p < 0.05$). Data are means ± SEM. (C and D) Endogenous acetylated Foxo3a proteins in the nuclei from control (si-Con) and *Sirt1*-knockdown HEI-OC1 cells (si-Sirt1) were isolated by immunoprecipitation with anti-acetyl-lysine antibody followed by Western blotting with anti-Foxo3a antibody (n = 3). (D) Quantification of the amount of total acetylated Foxo3a from (C). *Significantly different from control cells ($p < 0.05$). Data are means ± SEM. (E and F) Western blotting analysis of catalase and SOD_2 protein levels in control and *Sirt1*-knockdown HEI-OC1 cells. (F) Quantification of catalase and SOD_2 proteins levels from (E). (G) Catalase activities were measured in control and *Sirt1*-knockdown HEI-OC1 cells (n = 3). (H–M)

same housing and diet conditions and when compared on the same genetic background, Sirt1, but not Sirt3, promotes early onset of AHL in B6 mice. We note that recent findings support the antiaging effects of Sirt3 on hearing loss: activation of SIRT3 by the NAD^+ precursor, nicotinamide riboside protects from noise-induced hearing loss in mice (Brown et al., 2014), whereas there is a decrease in Sirt3 expression associated with accumulation of reactive oxygen species in the auditory cortex of an aging rat model (Zheng et al., 2014).

The C57BL/6J mouse strain is homozygous for the recessive AHL-susceptibility allele *Cdh23*^{753A} that is known to promote early onset of AHL by 12–15 months of age (Noben-Trauth et al., 2003). Hence, the mechanisms underlying early-onset of cochlear pathology and associated hearing loss in B6 mice might be different from the mechanisms underlying normal or late-onset AHL. To confirm that Sirt1 promotes AHL as our hearing and histologic analyses indicate, further studies are needed in *Sirt1*$^{+/-}$ mice in the background of a model of late-onset AHL such as the CBA/CaJ mouse strain, which does not carry the *Cdh23*^{753A} allele and does not display AHL until 17–20 months of age (Zheng et al., 1999). However, not only did we find that Sirt1 plays a key role in early-onset AHL in B6 mice, we also found Sirt1 is involved in regulation of antioxidant activity in cochlear cells and that *Sirt1* knockdown in HEI-OC1 cells results in increased resistance to oxidative stress. Therefore, we speculate that Sirt1 may also promote late-onset AHL in CBA/CaJ mice.

A recent study from the International Mouse Phenotyping Consortium (IMPC) showed that young mice homozygous for a *Sirt1* KO mutation exhibited significantly increased ABR thresholds compared with C57BL/6 control mice (https://www.mousephenotype.org/phenoview/?gid=363&qeid=MP:0004738&ctrl=2357729&pt=0.0001). A possible explanation for this contradicting result is that this was a preliminary screening test for auditory function using 2 young *Sirt1*$^{+/-}$ heterozygous mice (n = 2) and 2 young *Sirt1*$^{-/-}$ homozygous mice (n = 2) compared with C57BL/6 mice (n = 353) as controls. It is also possible that the *Sirt1*$^{-/-}$ homozygous mice tested at MRC Harwell exhibited higher ABR thresholds because of developmental defects in the inner ear and/or central nervous system since *Sirt1*$^{-/-}$ homozygous mice infrequently survive postnatally, exhibit development defects, and are small (Cheng et al., 2003). We acknowledge that because there are only a few reports on the role of Sirt1 in AHL in mice, further studies are needed to confirm the reports by the IMPC, Xiong et al., and our findings in middle-aged WT and *Sirt1*$^{+/-}$ heterozygous mice in the C57BL/6 background that are publicly available from IMPC or Jackson Laboratory.

Using transgenic mice with heart-specific overexpression of Sirt1 on the Friend leukemia virus B mouse background, Alcendor et al. have reported that high heart-specific overexpression of Sirt1 (12.5-fold) increased apoptosis and decreased cardiac function. However, the same report has shown that moderate heart-specific overexpression of *Sirt1* (2.5∼7.5-fold) protected the heart from oxidative stress induced by paraquat and increased catalase expression in mice (Alcendor et al., 2007). A possible explanation for the contradicting result is that because the cochlea is the receptor organ for hearing that is constantly exposed to noise and/or noise-induced oxidative stress throughout the life span and/or because B6 mice are more susceptible to age- and/or noise-related hair cell damage because of the *Cdh23* mutation, Sirt1 may act as a proaging molecule in the cochlear cells of B6 mice. Again, further studies are needed to confirm the report by Alcendor et al. as to how high- or moderate-inner ear-specific overexpression of *Sirt1* influences the progression of AHL in mice on the C57BL/6 background.

There are also a number of cell line and primary culture studies that support a protective effect of Sirt1 against oxidative stress. For example, Sirt1 inhibitors enhanced apoptosis and catalase expression, whereas *Sirt1* overexpression downregulated catalase in kidney cell lines (HK-2 cell lines; Hasegawa et al., 2008). Under hydrogen peroxide treatment, *Sirt1* overexpression also rescued H_2O_2-induced apoptosis through the upregulation of catalase and the nuclear accumulation of Foxo3a. In mouse myoblast cell lines, SIRT1 inhibitors increased antimycin A-induced reactive oxygen species levels and apoptosis (Hori et al., 2013). In addition, the SIRT1 activator resveratrol and NAD^+ suppressed apoptosis, whereas siRNA-mediated knockdown of *Sirt1* abolished those effects of resveratrol. In primary astrocytes derived from C57BL/6 mice, upregulation of Sirt1 induced by glucose deprivation increased the expression levels of SOD_2 and catalase, whereas inhibition of SIRT1 increased the acetylation of Foxo4, and decreased the expression levels of SOD_2 and catalase (Cheng et al., 2014). Furthermore, in cultured endothelial progenitor cells (EPCs) obtained from human umbilical cord blood, SIRT1 protein levels were increased by hydrogen peroxide, whereas hydrogen peroxide treatment dose-dependently induced apoptosis in EPCs (Wang et al., 2015). SIRT1 overexpression also reduced H_2O_2-induced apoptosis and decreased the total FOXO3a protein expression. Collectively, although those 4 studies were performed exclusively in cell lines or primary cultures, their results strongly support a protective effect of SIRT1 against oxidative stress. In the present study using mouse inner ear cell lines (HEI-OC1), we showed that *Sirt1* knockdown increased resistance to H_2O_2-induced cell death, catalase activity, and Foxo3a-mediated oxidative stress resistance, suggesting a role of Sirt1 in promoting oxidative stress. Our in vitro findings were verified and supported by in vivo tests, including ABR hearing tests, histopathologic analyses of cochlear tissues, and immunostaining of oxidative DNA damage marker, Sirt1, catalase, and Foxo3 proteins in the cochlear tissues of young and/or old WT and *Sirt1*$^{+/-}$ mice. A possible explanation for these contradicting results is that the role of Sirt1 in oxidative stress in the cochlear cells of B6 mice might be quite different from those in other cell types or other organs such as kidney cells, myocytes, astrocytes, and/or EPCs of other mouse strains because B6 mice are more susceptible to age- and/or noise-related hair cell damage due to the *Cdh23* mutation. Nevertheless, given that there are only a few reports on the roles of Sirt1 in oxidative stress in mouse inner ear cells lines or primary cochlear cultures, further studies are needed to verify our in vitro test reports and the other in vitro study reports.

4.2. Effects of Cdh23 genotype on the progression of AHL in KO and transgenic mice

The *Sirt1* KO mice used in the present study were derived from TC1 ES cells that were originated from the129/SvEvTacfBR strain (Deng et al., 1996) and were maintained on the 129/Sv substrain background (Cheng et al., 2003). There are a number of 129 substrains that exhibit extensive genetic variations due to admixtures

The numbers of catalase (Cat)-positive cells were counted in the OHCs (H and K), inner hair cells (I and L), and SGNs (J and M) in the apical (H–J) and middle (K–M) cochlear regions from WT and *Sirt1*$^{+/-}$ mice (n = 5) at 3 and 12 months of age. *Significantly different from age-matched WT mice ($p < 0.05$). Data are means ± SEM. Abbreviations: Cy, cytosol; IHC, inner hair cells; Mi, mitochondria; Nu, nuclear; OHC, outer hair cells; WT, wild-type.

with other strains during their derivations and subsequent genetic divergence (Simpson et al., 1997). In agreement with this report, 129P1/ReJ, 129P3/J, and 129X1/SvJ mice carry the *Cdh23*^{753A} allele, whereas 129S1/SvImJ, 129S6/SvEv-*Mos*^{tm1Ev}/J, and 129T2/SvEmsJ carry the *Cdh23*^{753G} allele (Johnson et al., 2006). To address the possible modifying effects that different 129 substrain backgrounds might have on hearing assessments of *Sirt1*$^{+/+}$ and *Sirt1*$^{+/-}$ mice on the B6 background that is homozygous for the recessive AHL-susceptibility allele *Cdh23*^{753A}, we sequenced the *Cdh23* gene in young *Sirt1*$^{+/+}$ and *Sirt1*$^{+/-}$ mice and confirmed that both the *Sirt1*$^{+/+}$ and *Sirt1*$^{+/-}$ mice used in this study have the same genotype for *Cdh23* (Fig. 1B). We note that when assessing auditory function in KO and/or transgenic mice, knowing which 129 substrain was used to generate the mutant and controlling for strain background effects are critical. For example, when a KO mouse line is backcrossed onto the B6 mouse that has the *Cdh23*$^{753A/753A}$ genotype or CBA/CaJ mouse that has the *Cdh23*$^{753G/753G}$ genotype, the mutant mouse could have the *Cdh23*$^{753G/753G}$ genotype, whereas its WT counterpart could have the *Cdh23*$^{753A/753A}$ genotype, depending on the original background of the mouse line and/or the location of the mutated gene (e.g., if the gene is located close to the *Cdh23* gene on Chromosome 10). Hence, to avoid any confounding results, it is critical to confirm that both the mutant and its WT control mice have the same *Cdh23* genotype (e.g., *Cdh23*$^{753A/753A}$, *Cdh23*$^{753G/753A}$, or *Cdh23*$^{753G/753G}$) when assessing auditory function. At last, although we assume all of the phenotypic differences observed between WT and *Sirt1*$^{+/-}$ mice are due to the effects of *Sirt1* genotypes, we acknowledge that there might still be other genetic variants from the 129 background strains that contribute to phenotypic differences in these animals.

4.3. Tissue homeostasis, supporting cells, and SIRT1/FOXO3a-mediated regulation of oxidative stress in damaged cochlea

When sensory hair cells die, nonsensory supporting cells play a key role in the maintenance of epithelial barrier integrity and preserving ion homeostasis (Gale and Jagger, 2010; Jagger et al., 2014). In nonmammalian vertebrates such as birds, when sensory hair cells die, the dying hair cells are eliminated. New hair cells arise from the adjacent nonsensory supporting cells and the spaces they formerly occupied are rapidly filled by the supporting cells. In the cochlea of mammals, when hair cell dies, there is no regeneration of sensory hair cells (Jagger et al., 2014; Taylor et al., 2012). The hair cell lesion is filled by the adjacent supporting cells, and the columnar epithelium is remodeled as a flat epithelium (Jagger et al., 2014; Taylor et al., 2012).

The loss of hair cells is thought to trigger repair responses within the adjacent supporting cells and those repair processes are dependent on gap junctional intercellular communication (Jagger et al., 2014). Gap junctions are sites of direct communication between adjacent cells and all cochlear supporting cells are directly connected to adjacent supporting cells with gap junctions that allow ions and small molecules to flow between the supporting cells (Forge et al., 2002; Jagger et al., 2014). In the present study, we have demonstrated that both Sirt1 and Foxo3a proteins reside in the supporting cells of the organ of Corti of the cochlea in B6 mice. Hence, we speculate that when OHCs become damaged or are lost in the cochlea of B6 mice, the dying hair cells may trigger repair responses within the adjacent supporting cells, which in turn activate Sirt1 through gap junctional communication. This may lead to Foxo3a inhibition in the supporting cells, which in turn results in increased oxidative stress within the dying OHCs, promoting the elimination of the dying cells from the epithelium. Hence, in B6 mice that are more susceptible to age- and/or noise-related hair cell damage due to the *Cdh23* mutation, Sirt1 may play a role in the repair or remodeling process of the epithelium when hair cells become damaged or are lost.

A large body of evidence indicates that Insulin/IGF-1 and FOXO signaling influence life span extension in response to dietary restriction in a variety of species (Fontana et al., 2010; Kenyon, 2010). Genetic variants of the FOXO family member FOXO3a have also been shown to be associated with human longevity (Flachsbart et al., 2009; Kuningas et al., 2007; Li et al., 2009). It is also well established that FOXO3a regulates oxidative stress resistance by directly binding to the promoters of the antioxidant genes encoding catalase or manganese SOD in a variety of species (Calnan and Brunet, 2008; Huang and Tindall, 2007). In agreement with these reports, overexpression of catalase (*Cat*) results in reduced age-related pathology in the heart, reduces cochlear pathology, delays the onset of AHL and increases life span in C57BL/6 mice (Schriner et al., 2005; Someya et al., 2009). Furthermore, catalase expression and activity are reduced in aged mouse brain (Mo et al., 1995). In contrast, catalase KO mice do not show any developmental defects or gross abnormalities (Ho et al., 2004), and lenses from these *Cat* KO mice do not show increased susceptibility to oxidative stress, suggesting that *Cat* deficiency is compensated by other antioxidant enzymes. Therefore, although catalase deficiency may be compensated by another antioxidant enzyme, we speculate that catalase overexpression or FOXO3a-mediated catalase activation may play a role in oxidative stress resistance in the cochlea of rodents and humans. At last, although we have demonstrated that Sirt1 can activate Foxo3a by promoting the translocation of Foxo3a to the nucleus and by increasing the acetylation status of nuclear Foxo3a in mouse inner ear cell lines, we acknowledge that these cell cultures test results are not verified in the cochlea of middle-aged WT and *Sirt1*$^{+/-}$ mice. Therefore, further research is needed to verify our in vitro test results and proposed hypothesis in the cochlea of B6 as well as CBA/CaJ mice.

Disclosure statement

The authors declare no competing financial interests.

Acknowledgements

This research was supported by National Institutes of Health (NIH) Grants RO1 AG021905 (Tomas A. Prolla), R01 DC012552 (Shinichi Someya), R01 DC014437 (Shinichi Someya), and R03 DC011840 (Shinichi Someya), and American Federation for Aging Research Grant 12388 (Shinichi Someya). The authors thank L. VanEkeris and S. Kinoshita for histological processing.

References

Alcendor, R.R., Gao, S., Zhai, P., Zablocki, D., Holle, E., Yu, X., Tian, B., Wagner, T., Vatner, S.F., Sadoshima, J., 2007. Sirt1 regulates aging and resistance to oxidative stress in the heart. Circ. Res. 100, 1512–1521.

Baur, J.A., Pearson, K.J., Price, N.L., Jamieson, H.A., Lerin, C., Kalra, A., Prabhu, V.V., Allard, J.S., Lopez-Lluch, G., Lewis, K., Pistell, P.J., Poosala, S., Becker, K.G., Boss, O., Gwinn, D., Wang, M., Ramaswamy, S., Fishbein, K.W., Spencer, R.G., Lakatta, E.G., Le Couteur, D., Shaw, R.J., Navas, P., Puigserver, P., Ingram, D.K., de Cabo, R., Sinclair, D.A., 2006. Resveratrol improves health and survival of mice on a high-calorie diet. Nature 444, 337–342.

Brown, K.D., Maqsood, S., Huang, J.Y., Pan, Y., Harkcom, W., Li, W., Sauve, A., Verdin, E., Jaffrey, S.R., 2014. Activation of SIRT3 by the NAD^{+} precursor nicotinamide riboside protects from noise-induced hearing loss. Cell Metab. 20, 1059–1068.

Burnett, C., Valentini, S., Cabreiro, F., Goss, M., Somogyvari, M., Piper, M.D., Hoddinott, M., Sutphin, G.L., Leko, V., McElwee, J.J., Vazquez-Manrique, R.P., Orfila, A.M., Ackerman, D., Au, C., Vinti, G., Riesen, M., Howard, K., Neri, C., Bedalov, A., Kaeberlein, M., Soti, C., Partridge, L., Gems, D., 2011. Absence of effects of Sir2 overexpression on lifespan in C. elegans and Drosophila. Nature 477, 482–485.

Calnan, D.R., Brunet, A., 2008. The FoxO code. Oncogene 27, 2276–2288.

Cheng, H.L., Mostoslavsky, R., Saito, S., Manis, J.P., Gu, Y., Patel, P., Bronson, R., Appella, E., Alt, F.W., Chua, K.F., 2003. Developmental defects and p53

hyperacetylation in Sir2 homolog (SIRT1)-deficient mice. Proc. Natl. Acad. Sci. U S A 100, 10794–10799.
Cheng, Y., Takeuchi, H., Sonobe, Y., Jin, S., Wang, Y., Horiuchi, H., Parajuli, B., Kawanokuchi, J., Mizuno, T., Suzumura, A., 2014. Sirtuin 1 attenuates oxidative stress via upregulation of superoxide dismutase 2 and catalase in astrocytes. J. Neuroimmunol. 269, 38–43.
Deng, C., Wynshaw-Boris, A., Zhou, F., Kuo, A., Leder, P., 1996. Fibroblast growth factor receptor 3 is a negative regulator of bone growth. Cell 84, 911–921.
Finkel, T., Deng, C.X., Mostoslavsky, R., 2009. Recent progress in the biology and physiology of sirtuins. Nature 460, 587–591.
Flachsbart, F., Caliebe, A., Kleindorp, R., Blanché, H., von Eller-Eberstein, H., Nikolaus, S., Schreiber, S., Nebel, A., 2009. Association of FOXO3A variation with human longevity confirmed in German centenarians. Proc. Natl. Acad. Sci. U S A 106, 2700–2705.
Fontana, L., Partridge, L., Longo, V.D., 2010. Extending healthy life span–from yeast to humans. Science 328, 321–326.
Forge, A., Becker, D., Casalotti, S., Edwards, J., Marziano, N., Nickel, R., 2002. Connexins and gap junctions in the inner ear. Audiol. Neurootol. 7, 141–145.
Frisina, D.A., Frisina, R.D., 1997. Speech recognition in noise and presbycusis: relations to possible neural mechanisms. Hear. Res. 106, 95–104.
Gale, J.E., Jagger, D.J., 2010. Cochlear supporting cells. In: Fuchs, P.A. (Ed.), The Oxford Handbook of Auditory Science: The Ear. Oxford UP, Oxford, pp. 307–327.
Gates, G.A., Mills, J.H., 2005. Presbycusis. Lancet 366, 1111–1120.
Hasegawa, K., Wakino, S., Yoshioka, K., Tatematsu, S., Hara, Y., Minakuchi, H., Washida, N., Tokuyama, H., Hayashi, K., Itoh, H., 2008. Sirt1 protects against oxidative stress-induced renal tubular cell apoptosis by the bidirectional regulation of catalase expression. Biochem. Biophys. Res. Commun. 372, 51–56.
Ho, Y.S., Xiong, Y., Ma, W., Spector, A., Ho, D.S., 2004. Mice lacking catalase develop normally but show differential sensitivity to oxidant tissue injury. J. Biol. Chem. 279, 32804–32812.
Hori, Y.S., Kuno, A., Hosoda, R., Horio, Y., 2013. Regulation of FOXOs and p53 by SIRT1 modulators under oxidative stress. PLoS One 8, e73875.
Huang, H., Tindall, D.J., 2007. Dynamic FoxO transcription factors. J. Cell Sci. 120 (Pt 15), 2479–2487.
Hudspeth, A.J., 1997. How hearing happens. Neuron 19, 947–950.
Jagger, D.J., Nickel, R., Forge, A., 2014. Gap junctional coupling is essential for epithelial repair in the avian cochlea. J. Neurosci. 34, 15851–15860.
Johnson, K.R., Zheng, Q.Y., Noben-Trauth, K., 2006. Strain background effects and genetic modifiers of hearing in mice. Brain Res. 1091, 79–88.
Kaeberlein, M., 2010. Lessons on longevity from budding yeast. Nature 464, 513–519.
Kalinec, G.M., Webster, P., Lim, D.J., Kalinec, F., 2003. A cochlear cell line as an in vitro system for drug ototoxicity screening. Audiol. Neurootol. 8, 177–189.
Keithley, E.M., Canto, C., Zheng, Q.Y., Wang, X., Fischel-Ghodsian, N., Johnson, K.R., 2005. Cu/Zn superoxide dismutase and age-related hearing loss. Hear. Res. 209, 76–85.
Kenyon, C.J., 2010. The genetics of ageing. Nature 464, 504–512.
Kuningas, M., Mägi, R., Westendorp, R.G., Slagboom, P.E., Remm, M., van Heemst, D., 2007. Haplotypes in the human Foxo1a and Foxo3a genes; impact on disease and mortality at old age. Eur. J. Hum. Genet. 15, 294–301.
Li, Y., Wang, W.J., Cao, H., Lu, J., Wu, C., Hu, F.Y., Guo, J., Zhao, L., Yang, F., Zhang, Y.X., Li, W., Zheng, G.Y., Cui, H., Chen, X., Zhu, Z., He, H., Dong, B., Mo, X., Zeng, Y., Tian, X.L., 2009. Genetic association of FOXO1A and FOXO3A with longevity trait in Han Chinese populations. Hum. Mol. Genet. 18, 4897–4904.
Li, Y., Xu, W., McBurney, M.W., Longo, V.D., 2008. SirT1 inhibition reduces IGF-I/IRS-2/Ras/ERK1/2 signaling and protects neurons. Cell Metab. 8, 38–48.
Lin, S.J., Defossez, P.A., Guarente, L., 2000. Requirement of NAD and SIR2 for life-span extension by calorie restriction in Saccharomyces cerevisiae. Science 289, 2126–2128.
Merchant, S.N., Nadol, J.B., 2010. Schuknecht's Pathology of the Ear, third ed. PMPH, USA.
Mo, J.Q., Hom, D.G., Andersen, J.K., 1995. Decreases in protective enzymes correlates with increased oxidative damage in the aging mouse brain. Mech. Ageing Dev. 81, 73–82.
Motta, M.C., Divecha, N., Lemieux, M., Kamel, C., Chen, D., Gu, W., Bultsma, Y., McBurney, M., Guarente, L., 2004. Mammalian SIRT1 represses forkhead transcription factors. Cell 116, 551–563.
Noben-Trauth, K., Zheng, Q.Y., Johnson, K.R., 2003. Association of cadherin 23 with polygenic inheritance and genetic modification of sensorineural hearing loss. Nat. Genet. 35, 21–23.
Pugh, T.D., Klopp, R.G., Weindruch, R., 1999. Controlling caloric consumption: protocols for rodents and rhesus monkeys. Neurobiol. Aging 20, 157–165.
Rogina, B., Helfand, S.L., 2004. Sir2 mediates longevity in the fly through a pathway related to calorie restriction. Proc. Natl. Acad. Sci. U S A 101, 15998–16003.
Schriner, S.E., Linford, N.J., Martin, G.M., Treuting, P., Ogburn, C.E., Emond, M., Coskun, P.E., Ladiges, W., Wolf, N., Van Remmen, H., Wallace, D.C., Rabinovitch, P.S., 2005. Extension of murine life span by overexpression of catalase targeted to mitochondria. Science 308, 1909–1911.
Simpson, E.M., Linder, C.C., Sargent, E.E., Davisson, M.T., Mobraaten, L.E., Sharp, J.J., 1997. Genetic variation among 129 substrains and its importance for targeted mutagenesis in mice. Nat. Genet. 16, 19–27.
Someya, S., Xu, J., Kondo, K., Ding, D., Salvi, R.J., Yamasoba, T., Rabinovitch, P.S., Weindruch, R., Leeuwenburgh, C., Tanokura, M., Prolla, T.A., 2009. Age-related hearing loss in C57BL/6J mice is mediated by Bak-dependent mitochondrial apoptosis. Proc. Natl. Acad. Sci. U S A 106, 19432–19437.
Someya, S., Yu, W., Hallows, W.C., Xu, J., Vann, J.M., Leeuwenburgh, C., Tanokura, M., Denu, J.M., Prolla, T.A., 2010. Sirt3 mediates reduction of oxidative damage and prevention of age-related hearing loss under caloric restriction. Cell 143, 802–812.
Spongr, V.P., Flood, D.G., Frisina, R.D., Salvi, R.J., 1997. Quantitative measures of hair cell loss in CBA and C57BL/6 mice throughout their life spans. J. Acoust. Soc. Am. 101, 3546–3553.
Taylor, R.R., Jagger, D.J., Forge, A., 2012. Defining the cellular environment in the organ of Corti following extensive hair cell loss: a basis for future sensory cell replacement in the Cochlea. PLoS One 7, e30577.
Tissenbaum, H.A., Guarente, L., 2001. Increased dosage of a sir-2 gene extends lifespan in Caenorhabditis elegans. Nature 410, 227–230.
Viswanathan, M., Kim, S.K., Berdichevsky, A., Guarente, L., 2005. A role for SIR-2.1 regulation of ER stress response genes in determining C. elegans life span. Dev. Cell 9, 605–615.
Wang, Y., Tissenbaum, H.A., 2006. Overlapping and distinct functions for a Caenorhabditis elegans SIR2 and DAF-16/FOXO. Mech. Ageing Dev. 127, 48–56.
Wang, Y.Q., Cao, Q., Wang, F., Huang, L.Y., Sang, T.T., Liu, F., Chen, S.Y., 2015. SIRT1 protects against oxidative stress-induced endothelial progenitor cells apoptosis by inhibiting FOXO3a via FOXO3a Ubiquitination and Degradation. J. Cell Physiol. 230, 2098–2107.
Weindruch, R., Sohal, R.S., 1997. Seminars in medicine of the Beth Israel Deaconess Medical center. Caloric intake and aging. N. Engl. J. Med. 337, 986–994.
Xiong, H., Dai, M., Ou, Y., Pang, J., Yang, H., Huang, Q., Chen, S., Zhang, Z., Xu, Y., Cai, Y., Liang, M., Zhang, X., Lai, L., Zheng, Y., 2014. SIRT1 expression in the cochlea and auditory cortex of a mouse model of age-related hearing loss. Exp. Gerontol. 51, 8–14.
Xiong, H., Pang, J., Yang, H., Dai, M., Liu, Y., Ou, Y., Huang, Q., Chen, S., Zhang, Z., Xu, Y., Lai, L., Zheng, Y., 2015. Activation of miR-34a/SIRT1/p53 signaling contributes to cochlear hair cell apoptosis: implications for age-related hearing loss. Neurobiol. Aging 36, 1692–1701.
Yamasoba, T., Lin, F.R., Someya, S., Kashio, A., Sakamoto, T., Kondo, K., 2013. Current concepts in age-related hearing loss: epidemiology and mechanistic pathways. Hear. Res. 303, 30–38.
Zheng, L., Yang, Y., Hu, Y., Sun, Y., Du, Z., Xie, Z., Zhou, T., Kong, W., 2014. Age-related decrease in the mitochondrial sirtuin deacetylase Sirt3 expression associated with ROS accumulation in the auditory cortex of the mimetic aging rat model. PLoS One 9, e88019.
Zheng, Q.Y., Johnson, K.R., Erway, L.C., 1999. Assessment of hearing in 80 inbred strains of mice by ABR threshold analyses. Hear. Res. 130, 94–107.